**Original article**
https://doi.org/10.18019/1028-4427-2025-31-6-780-797

# Stress and strain of the radial shaft with marginal notch and compensating elements explored with computer modelling

**N.M. Aleksandrov[1]✉, V.D. Veshutkin[2], A.E. Zhukov[2], I.D. Veshaev[1]**

[1] Privolzhsky Research Medical University, Nizhny Novgorod, Russian Federation
[2] Nizhny Novgorod State Technical University named after R.E. Alekseev, Nizhny Novgorod, Russian Federation

**Corresponding author**: Nikolay M. Aleksandrov, aleksandrov-chetai@rambler.ru

**Abstract**

**Introduction** The incidence of pathological fracture of the radius at the site of a marginal defect following graft harvesting reaches 31 %. A finite element computer simulation model allows for non-invasive determination and prediction of the stress and strain (SS) of the bone, the strength and susceptibility to fracture under various loads and strengthening methods.

The **objective** was to present the results of the finite element analysis on the influence of various marginal notch shapes, bone curvature and methods for increasing the strength on the SS of the radial shaft.

**Material and methods** Based on anatomical preparations of the human radius, solid-state linear-elastic modeling of the entire cortical diaphysis of the radius was performed including the shaft with rectangular and triangular marginal notches, curvature in two planes using different reinforcing plates and fixation methods under non-destructive tensile, compressive, torsional and bending loads. The longitudinal stability of the bone was determined. ANSYS and NX Siemens software packages were used in the study.

**Results** A triangular cutout reduced bone stress by 21.4 % in tension and by 51.5 % in torsion as compared to a rectangular cutout increasing the longitudinal stability margin by 1.18 times. Bi-planar bone curvature increased stress and reduced the tensile load-bearing capacity by 2.89 times. A 2 mm thick semi-tubular plate, compared to a flat narrow plate of similar thickness and 10 mm width reduced the level of maximum stresses in the bone model by 1.2–1.5 times in tension and by 3.5–3.9 times in torsion for different cutouts. Measurements of longitudinal stability for a semitubular plate increased critical stresses by 1.3–1.5 times for different osteotomies as compared to a bone without a cutout and plate.

**Discussion** With all the loads, the strength conditions of the bone model with a cutout were provided when fixed with a plate at least 2 mm thick on four 2.0 mm bicortical screws inserted two distally and two proximally to the cutout.

**Conclusion** The findings demonstrated practical use of bone plates reducing SS of the radius with any cutout.

**Keywords**: radial bone-cutaneous flap, marginal defect of the radius, stress and strain of the bone, notch compensation, strength of the radius, computer modelling

**For citation**: Aleksandrov NM, Veshutkin VD, Zhukov AE, Veshaev ID. Stress and strain of the radial shaft with marginal notch and compensating elements explored with computer modelling. *Genij Ortopedii*. 2025;31(6):780-797. doi: 10.18019/1028-4427-2025-31-6-780-797.

## INTRODUCTION

A radial forearm free flap (RFFF) is used in reconstructive surgery to replace tissue defects [1, 2]. With its obvious advantages, this method is associated with the morbidity of the donor site and cannot be widely used. Harvesting the graft for transfer or relocation to the recipient site results in the formation of a marginal defect in the radial shaft. The incidence of pathological fracture of the radius at the marginal defect reaches 31 % [3, 4]. Treatment of the complication which causes functional and cosmetic impairment of the hand and forearm, presents a surgical challenge and requires lengthy treatment periods and significant financial costs. Experts' opinions on methods for preventing the complications remain controversial. There are conflicting opinions in the literature regarding the influence of the shape of the marginal notch on the strength of the radius: from complete denial to a significant weakening effect [5, 6]. Most authors recognize the role of prophylactic fixation of the donor radius [7, 8, 9]. Analysis of the works on the topic shows that many issues remain debatable, and the opinions of specialists are contradictory [10]. There are no publications reporting the effect of different osteotomies on bone strength; fixation methods, types of metal plates, the number, diameter of screws, their placement for fixing the plate to the bone have not been substantiated; mechanisms of loosening the screws have not been explored. Most authors evaluate residual bone strength and select a method for fracture prevention based on clinical and radiological data [11, 12]. An effect of the factors on bone strength is essential for development and substantiation of the methods for its strengthening and prevention of pathological fractures. Evolution of software and computer technology facilitated high reliability (95–99 %) and clarity in simulating the behavior of a product under the influence of various loads, including mechanical loads, and probabilistic assessment of the reliability of the constructs [13, 14]. The finite element method (FEM) is one of the most common methods for solving problems in mechanics including biomechanics [15]. The finite element model (FEM) is the bone model for the numerical solution of strength problems in biomechanics [15]. The level of internal mechanical stress is one of the key parameters that must be determined to assess a material's strength. A finite element computer simulation model allows for non-invasive determination and prediction of bone's mechanical response for various loads and predisposition (susceptibility) to destruction at the site of maximum mechanical stresses under loads, provides clarity, visualization, and accessibility of analysis of the parameters of the entire object [16, 17]. The advantages of FEM include the possibility to explore structures composed of several materials of any shape, and the feasibility of considering various boundary conditions [18, 19]. According to the literature, FEM allows us to determine the strength of the radius, examine the stability of orthopedic implants, which facilitates the implementation of measures to prevent fractures [20]. The available literature contains rather contradictory data obtained by computer modeling methods regarding the mechanical properties of the radial bones with various forms of marginal osteotomy, methods of compensating for the resulting defects, fixation of the plate and strengthening of the bone under tension, compression, bending and torsion [21, 22]. There are no publications reporting the influence of bone curvature on its strength. The choice of the type of plate, the number and size of screws, the nature of their implementation from the standpoint of bone stress and strain (SS), are not sufficiently substantiated, the longitudinal stability of the model with a cutout and a plate has not been studied [23, 24], and this is a limiting factor in the development of methods for preventing pathological fractures. Therefore, knowledge of the nature of stress distribution in intact bone and after the formation of a marginal notch, in the *bone-fixator* system, is necessary to adequately determine the method of preventive bone strengthening.

The **objective** was to present the results of the finite element analysis on the influence of various marginal notch shapes, bone curvature and methods for increasing the strength on the SS of the radial shaft.

## MATERIAL AND METHODS

3D models of the radial shaft were created using a CAD computer-aided design system:

— without cutout and initial deflection;

— without a cutout with an initial bend in one (horizontal or vertical) or two planes;

— with a triangular cutout and an initial bend in one or two planes;

— with a rectangular cutout and an initial bend in one or two planes,

— with similar cutouts and bends with bone flat and semi-tubular plates fixed with two, four and six screws of different lengths and diameters;

— with a rectangular cutout and a compensating insert fixed with two screws.

Models of a *screw–bone* pair were created in a similar manner with a rectangular cutout replaced by a cortical insert of identical shape and size, fixed with screws and reinforced with a bone plate.

FEM calculations were performed using ANSYS and Siemens NX software packages to measure stresses. To simplify the calculations, the bone tissue of the radial shaft was assumed to be solid, homogeneous, linear, elastic (linear-elastic), continuous, and isotropic. It is accepted that compact bone is isotropic, since it has a common lamellar and relatively homogeneous structure, and the characteristics of strength and elasticity do not change in the radial shaft.

Measurements included the volumetric dynamic non-destructive loading SS on a linear-elastic isotropic hybrid model of the radial shaft, obeying the generalized Hooke's law, in compliance with the hypotheses of the technical theory of beam bending, since the graft is mostly harvested from this part of the bone in the clinic.

SS was assessed on the basis of the third and fourth theories of strength using the von Mises criterion providing an idea of the overall stress intensity and also combines the normal and shear stresses acting on the object. The choice of this criterion used to characterize the properties of a viscous material, is due to the use of metal compensating elements (plate, screws) in the model.

The parameters effecting the maximum bone stress were examined to include the shape and depth of the cut, the curvature of the bone in one or two different planes, the nature of the defect compensation, the type of plate, its dimensions (width, length, thickness), number of plates, the methods of insertion and the size of the screws fixing the plate to the bone with a rectangular and triangular cutout.

Critical stresses were tested for longitudinal stability of the bone. A spatial geometric model of the bone was constructed in the first stage of the study, then the model was broken down into finite elements (FEs) using a finite element mesh generator program. The complex three-dimensional geometry of the radial diaphysis and the analysis of the construction and behavior of various CEMs determined the choice of a three-dimensional CEM of the bone.

A 10-node second-order isoparametric tetrahedral element (CTetra 10) was used as the finite element type to form a volumetric solid mesh. The elements had three degrees of freedom at each node. Movement along the coordinate axes was optimal for displaying irregularly shaped objects with complex geometry in the software packages used.

Sections of anatomical specimens of the radius were used to construct a three-dimensional linear FEM model. The geometric calculation model consisted of a cylindrical structure with a cross-section composed of a semicircle and two lateral trapezoids symmetrical about a common axis. The geometry of the bone section and the initial curvature of the bone in two planes corresponded to the actual average dimensions obtained experimentally on cadaver (anatomical) material.

The physical characteristics of the model materials were specified in the second stage. The elastic moduli and Poisson's ratios of the various materials used in the calculations were taken from literature sources or obtained experimentally.

The mechanical properties adopted for bone material included Young's modulus of $0.2\times10^5$ MPa, Poisson's ratio (transverse deformation coefficient) of 0.3, tensile strength of 120 MPa, and density $\rho = 2400$ kg/m$^3$. For plates and screws made of VT6 titanium, Young's modulus measured $1.15\times10^5$ MPa, and Poisson's ratio was 0.32. The friction coefficient μ for the *metal-to-metal* contact pair was taken to be 0.15, and for the *bone-to-metal* pair, 0.3. The permissible normal tensile stresses of 60 MPa were taken from the condition of 0.5 of the ultimate strength (two times the safety factor). For torsion, the permissible shear stress was generally taken to be 0.5 times the normal stress (in accordance with the third strength hypothesis, i.e., 0.25 times the ultimate strength). In our cases, approximately 0.2 times the ultimate strength was adopted. The relative depth of the triangular and rectangular notches $h_0/H$ was 0.16 and 0.33 (H being the height of the section of the intact bone, $h_0$ being the depth of the notch).

Bone deflection was modeled in two directions: x = 3.73 mm; y = 6.38 mm. A *screw-bone* pair was simulated. Simplified models of fixators of varying thickness (1 mm, 2 mm, 2.5 mm, 3 mm) were created for a flat reconstructive plate, a semitubular plate, and fixation screws; and screw models with diameters of 2 mm, 3.5 mm and 4.5 mm, lengths of 4 mm, 13 mm and 18 mm, were constructed according to their real dimensions. The number of elements in the model varied from 21,351 to 51,157, the number of nodes from 37,763 to 82,186, and the element sizes from 4.98 mm to 0.2 mm, depending on the size, nature, and characteristics of the simulated object and its objectives. The smallest finite element size and the largest number of nodes were used to model the screw and its connection to the bone. The mesh was thickened in areas where stress concentration was expected, in areas of thinning of the cortical plate and in areas with complex geometry.

Tension, compression (longitudinal stability, longitudinal bending, longitudinal deformation), torsion and complex loading (tension and bending) were examined. Bones subjected to compression can undergo longitudinal bending under load, and the bone model was tested for stability. The following boundary conditions were set. A rigid clamp was installed along the cross-sectional surface at one free end of the bone. Movement along all planes was ruled out, while uniform pressure or torque was applied to the other end along the cross-sectional plane.

A load was applied to the bone model in the third stage. Depending on the model type and the study objective, the static physiological load on the bone was 981 N, 800 N, or 400 N for tension and compression, and always 0.1 Nm for torsion. The load of 981 N applied corresponds to the weight of an average male. A load of 400 N was used to simplify calculations and determine changes in stress field boundaries and maximum stress values more accurately.

When the bone interacts with the metal plate, forces from the bone are transmitted to the plate by the screws. Since the plate prevents longitudinal deformation of the bone under load, the screw is primarily subject to shear forces. Furthermore, the bone's curvature causes bending stresses during tension and axial loads on the screw. For this reason, factors influencing the strength of screw fixation in bone were examined under axial and tangential loads on the screw head inserted outside the plate. When studying the stress in *screw-cortical bone* contact pairs (at the screw-bone interface), the bone was secured at both ends using rigid fixation. The magnitude of the tangential load was 100 N, and the axial load was 50 N, 100 N, 150 N. The stress values in the plate and screws were used as an additional criterion.

A qualitative and quantitative assessment of the stress fields of intact bone was performed after the formation of cutouts of various shapes and sizes with curvature in various planes without defect compensation and after prophylactic bone strengthening. The magnitude and zone of maximum stress concentration in various sections of the cutout of the shaft, plate and screws, the change in the area of the zone of maximum stress concentration under compression-tension and torsion were determined depending on the shape, depth of the cut, the curvature of the bone in two planes and the methods of its preventive strengthening with a metal plate on screws.

Bone stress values were chosen as the criterion for evaluating the effectiveness of the fixation plate. The use of FEM allowed us to identify and describe areas of local stress concentration, and explore their quantitative values and gradients within and across the bone surface.

## RESULTS

The SDS of the bone model without cutouts or curvatures was characterized by a smooth distribution of the parameters across the model's surface, with no sharp changes. This bone model had no areas of stress concentration during tension and compression. Tensile stresses were uniformly distributed, and their values were the lowest of all the calculated cases considered. When stretching a bone model with vertical curvature, peak stresses were determined at the interosseous margin, and for a horizontal curvature, at the anterior margin. The presence of bone curvature in two planes under tensile conditions resulted in the occurrence of bending stresses also in two planes (Fig. 1). In these cases, peak stress areas were located in the interosseous and posterior margins of the radius. The area of increased stress during torsion of bone models with curvature was located along the anterior edge and the anterior surface of the bone.

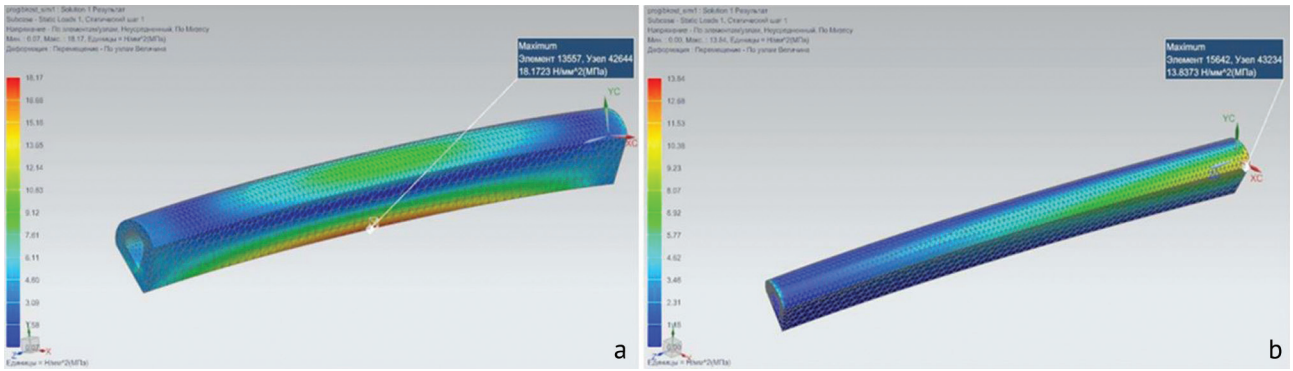


**Fig. 1** Distribution of equivalent stresses according to von Mises in a bone without a notch with an initial deflection in two directions: (a) under tension; (b) under torsion

The bone model with curvature and a notch experienced the greatest stress in the notch area under all loading conditions. Areas of stress concentration were observed in areas with geometric changes. The formation of the notch caused stress concentrations in the corners of the triangular and rectangular notches and increased stress levels across the entire horizontal portion of the rectangular notch and the anterior surface of the bone under all types of loading. As the notch depth increased, peak stresses and their distribution area also increased under tension and torsion for all types of bone curvature. As expected, maximum tensile, compressive, and torsional stresses were observed at the location where the bone model's cross-section was minimal. In the presence of bone curvature and a notch, the stress distribution was non-uniform. When stretching and having a bend in the bone in the horizontal plane, the maximum stress was noted along the front edge of the notch of any shape.

When bending the bone in the vertical plane, maximum stress was observed in the interosseous margin area for any cutout shape. When bending the bone model in two planes, pronounced stress concentrations were observed in the following areas:

— interosseous margin of the bone in the zone of maximum deflection;

— in the corner of the triangular cutout along the back edge (under stretching-compression);

— across the entire plane or along the rear edge of the longitudinal part of the rectangular cutout, depending on its depth (Fig. 2, 3).

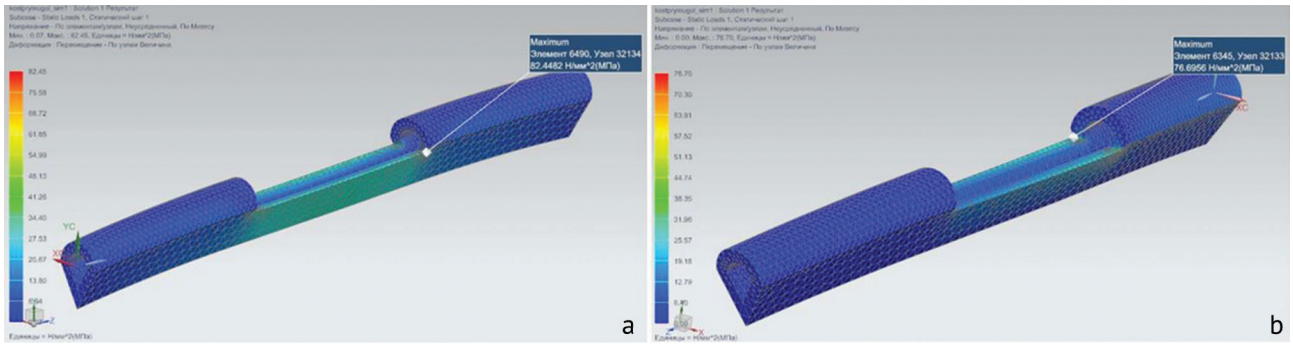


**Fig. 2** Distribution of equivalent stresses according to von Mises in a bone with a rectangular notch and with an initial deflection in two directions: (a) under tension; (b) under torsion

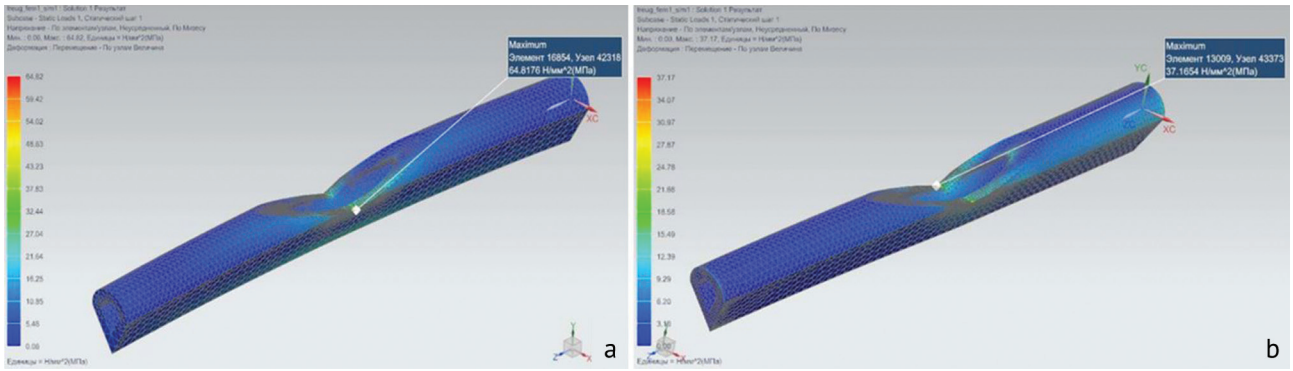


**Fig. 3** Distribution of equivalent stresses according to von Mises in a bone with a triangular notch and with an initial deflection in two directions: (a) under tension; (b) under torsion

During torsion, stress concentrations were noted in the area of the notch: for a triangular notch, at the corner of the notch; for a rectangular notch, across the entire plane or along the edges of the longitudinal portion of the notch, depending on its depth. The zone of greatest stress along the length of the bone for a triangular notch was significantly smaller than for a rectangular notch, both under tension and torsion.

The calculations showed that the structural shape of the cutout, which ensures the greatest load perception during tension and torsion, has a triangular shape with a depth of $h_0/H = 0.16$ (where $h_0$ is the depth of the cutout, H is the height of the bone section without the cutout). As the depth of the bone cut with curvature increased to $h_0/H = 0.33$, the peak values of maximum stresses increased for all cut shapes.

Table 1

Equivalent von Mises stresses in bones of different shapes under tension and torsion

| Types of loading | von Mises stresses depending on bone shape, MPa | | | |
|---|---|---|---|---|
| | without cutout and initial deflection | without cutout with initial dent | with a triangular cutout and an initial bend | with a rectangular cutout and an initial bend |
| Stretching, F = 400 N | 6.28 | 18.17 | 64.82 | 82.45 |
| Torsion, M = 0,1 N·m | 12.93 | 13.84 | 37.17 | 76.70 |

As Table 1 shows, the bone without the notch and initial curvature experiences the lowest stress. The presence of initial curvature increases the stress by 2.89 times in tension and only 1.1 times in torsion compared to the bone model without the notch. Based on the results, it can be concluded that the highest stresses were observed with a rectangular notch and initial bone deflection in both directions under all types of loading. For the same notch depth, a triangular shape is preferable to a rectangular one, as it produces lower stress levels under the same loading. The stress of the triangular notch is 78.6 % of the stress of the rectangular notch in tension and 48.5 % in torsion, that is, the triangular notch reduces the stress level by 21.4 % in tension and 51.5 % in torsion.

The presence of bone curvature causes increased tensile stress in the model without damage by 2.89 times due to the appearance of stress from bending, in conditions of its combination with a triangular cutout — by 10.32 times, with a rectangular cutout — by 13.13 times compared to the model without curvature and cutout. Bone curvature increases the torsional stress level by 1.1 times in the absence of damage, 2.88 times with a triangular notch, and 5.93 times with a rectangular notch (Table 1). The stresses caused by the presence of the notch and bone curvature are summed up.

The results of the analysis of the bone model behavior under compressive load showed that the model under a load of 981 N cannot operate without loss of stability under any type of artificial cut, since the critical stresses for the first form of lost stability were an order of magnitude lower than the maximum stresses identified for a given load, in contrast to the model without a cutout. The model with a triangular cutout had a greater margin of safety for longitudinal stability (1.18 times) compared to the model with a rectangular cutout (Table 2).

Table 2

Stresses acting in samples with different cuts when solving the problem of longitudinal stability

| Bone shape | Stress σ, MPa | |
|---|---|---|
| | $\sigma_{max}$ | $\sigma_{cr}$ for the first form of lost stability |
| No cutout | 31.76 | 54.18 |
| Rectangular cutout | 47.60 | 39.96 |
| Triangle cutout | 59.23 | 46.99 |

A review of the literature shows that narrow plates are most often used for osteosynthesis in practice. Due to this and the fact that bone with a triangular notch and plate was found to be stronger in most respects than bone with a rectangular notch and plate, only the strengthening variant of bone with a triangular notch was further investigated. The bone model with a cutout and a plate and the plate in the defect projection showed greater stress in the defect area under all types of loading, cutout, and deflection. Stress concentrators arose at the points of geometric changes, as well as at the contact points between the parts (Fig. 4).

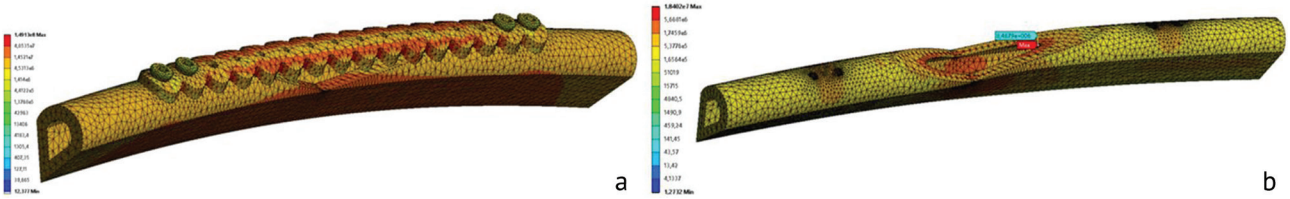


Fig. 4 Distribution of the von Mises equivalent stress in a bone with a triangular notch under compression (four screws, plate thickness 2 mm): (a) general distribution in the model, (b) distribution in the bone

The stresses along the plate's length between the screws in the notch area were distributed almost uniformly across the plate's width and concentrated between the screws. Beyond the screws, the stresses in the cantilevered areas were zero. The highest bone stresses were observed in the screws closest to the notch. With a through screw placement, zones of increased stress were identified in the area where the screws exited, which were more pronounced in the screws located next to the defect.

The criterion for assessing the effectiveness of the plate included the reduction in stress in the bone with the overlay in relation to the stress in the bone without the overlay. In models with a rectangular cutout replaced by a cortical insert of identical shape and size, fixed with screws and reinforced with a bone plate, the maximum stress during stretching was noted in the plate at the level of the corner of the cutout. The area of maximum bone stress was determined at the interosseous margin at the same level. When fixing the insert with screws alone, the areas of maximum bone stress were observed at the corners of the notch and at the interosseous margin at the same levels. In this model, the use of the plate reduced the maximum bone stress by 2.21 times.

When the model is stretched, the stress level in the bone would depend on the plate thickness and the number of screws (Fig. 5). The stress exceeded the permissible values under the conditions using a 1 mm thick plate. Compared to this calculated case, a decrease in stress was observed in the bone model with a 2 mm thick plate. A direct relationship between stress reduction and the number of screws was also noted. The acceptable stress level was achieved by modeling a 2 mm thick plate on four screws with monocortical insertion. The strength requirement was met when using a 2 mm thick plate. An inverse relationship was observed between the stress values and the plate thickness. The strength condition was also met when using a 3 mm thick plate. A decrease in stress was observed in the bone model with a 3 mm thick plate compared to the model with a 2 mm thick plate.

It can be concluded that a 3 mm thick plate was most effective in terms of maximum stress. To conserve material, a 2 mm thick plate can be employed, as the calculated equivalent stresses in the bone do not exceed the tensile strength and differ only slightly from those in the bone model with a 3-mm-thick plate. The stresses in a 2-mm-thick plate using four screws differ insignificantly from those using six screws. The stresses in a 2 mm thick plate using four screws differ insignificantly from those using six screws. Therefore, using a 2 mm thick plate with four screws can be sufficient, as using plates with more screws in a clinical setting is more traumatic. The lowest stress in the bone was observed with use of a 3 mm thick plate on six fixing screws, therefore this fixation system is desirable in the presence of a pronounced bend and an increase in the depth of the cut of more than half the bone with the stress increasing sharply in it.

As the graph shows, increasing the number of screws has no effect on bone stress during torsion (Fig. 5). Increasing the plate thickness reduces bone stress under all types of loads. Stress within the plate also decreases with increasing plate thickness, and at 3 mm, the number of fixation screws has little effect.

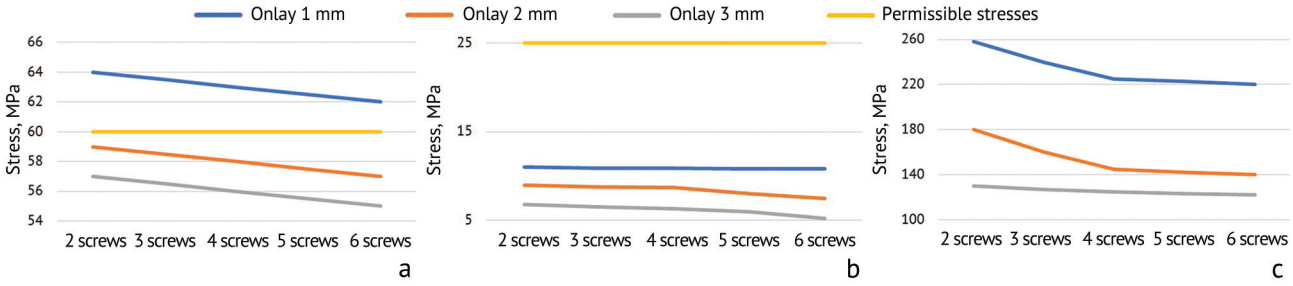


**Fig. 5** Graphs of the dependence of equivalent stresses on the plate thickness and the number of fixing screws: (a) in the bone under tension; (b) in the bone under torsion; (c) in the plate under tension

The stress distribution in the plate-bone-screw system was examined on a bone model with a triangular cutout and a plate on two screws with different plate thicknesses under tension (Table 3) and torsion (Table 4). Based on the results of the calculations performed under tension and torsion, it can be concluded that the stress in the plate, bone, and screw is linearly related to plate thickness. As plate thickness increases, stress decreases in each element of our working plate-bone-screw model. The highest concentration was found in the plate, suggesting that it could absorb most of the loads arising from bone extension and torsion. The lowest stresses were found in the screw.

Table 3

Values of equivalent stresses according to von Mises depending on the plate thickness under tension with a load of F = 980 N

| Plate thickness, mm | Stress σ, MPa | | |
|---|---|---|---|
| | in the plate | in the bone | in the screw |
| 2.0 | 154.69 | 121.48 | 46.00 |
| 2.5 | 126.16 | 111.34 | 30.20 |
| 3.0 | 124.93 | 110.49 | 23.89 |

Table 4

Values of equivalent stresses according to von Mises depending on the thickness of the plate under torsion with a load of M = 0.1 N·m

| Plate thickness, mm | Stress σ, MPa | | |
|---|---|---|---|
| | in the plate | in the bone | in the screw |
| 2.0 | 58.32 | 19.43 | 13.07 |
| 2.5 | 55.62 | 16.80 | 12.70 |
| 3.0 | 52.88 | 14.77 | 10.31 |

The plate played a key role under all types of loads, relieving the bone tissue. The screws absorbed the stress in the bone and transferred it to the plate. Regardless of the plate thickness, the stress in the bone did not exceed the tensile strength, and it did not even exceed the permissible stress under torsional stress. This was due to the fact that the plate reduced the angle of torsion due to its rigidity, thereby reducing the level of stress in the bone to a greater extent than with stretching.

The calculation of bone models for longitudinal stability was produced for artificial injuries of rectangular and triangular shape with a relative cut depth $h_0/H = 0.33$, with a deflection $f_x$ and $f_z$, with the immersion of six screws fixing a semi-tubular plate 2 mm thick to the bone, to a depth of 13 mm. The analysis of the results of the influence of bone strengthening with a plate on longitudinal stability is presented in Table 5.

Table 5

Destructive and critical loads acting on bones with notches

| Strength indicators | | Load values | | | | |
|---|---|---|---|---|---|---|
| | | no cutout | rectangular cutout | triangular cutout | rectangular cutout with plate | triangular cutout with plate |
| Stretching | $\sigma_{str}$, MPa | — | 47.60 | 44.44 | 41.95 | 39.68 |
| | $P_{destr}$, N | — | **2473** | **2649** | **2806** | **2967** |
| Compression | $\sigma_{str}$, MPa | 31.76 | 47.60 | 44.44 | 30.61 | 30.51 |
| | $P_{destr}$, N | 3706 | **2473** | **2649** | **3846** | **3858** |
| | $K = P_{cr}/P_{str}$ | –1.219 | –3.544 | –4.057 | –5.128 | –5.425 |
| | $P_{cr}$, N | **4238** | **3477** | **3980** | **5030** | **5322** |

The design load $P_{str}$ is assumed to be 981 N, and the failure load $P_{destr}$ is calculated upon reaching the ultimate strength of $\sigma_g = 120$ MPa. The failure load of the bone without the notch exceeds the design load by 3.78 times, which is the load safety factor. Calculations showed that the critical load of a defective bone is 1.4–1.5 times higher than the failure load. Bone failure will occur due to compression, not buckling. The plate increases the critical load by 1.45 times for a rectangular notch and by 1.34 times for a triangular notch, and also increases the breaking load for a rectangular cutout by 1.56 times, and for a triangular cutout by 1.46 times. The critical and maximum stresses in the bone are presented in Table 6.

Table 6

Critical and maximum stresses acting in specimens with different notch shapes and semi-tubular plates under compression

| Type of the bone cut with the plate | Stress, MPa | |
|---|---|---|
| | maximum $\sigma_{max}$ | critical $\sigma_{cr\,1}$ |
| rectangular cutout | 30.61 | 58.08 |
| triangular cutout | 30.51 | 61.55 |

Data analysis shows that the bone model with a metal plate under a design load of 981 N can operate without loss of stability under any type of artificial cut, since the critical stresses for the first form of lost stability appeared to be twice as high as the identified maximum stresses under the design load.

A comparative analysis of the effectiveness of the influence on stress in a bone model with different cutouts with a relative depth of $h_0/H = 0.33$, with a deflection of $f_x$ and $f_z$, a flat narrow and semi-tubular plate with a thickness of 2 mm and the immersion of six fixing screws to a depth of 13 mm was produced (Table 7).

A semi-tubular plate, compared to a flat narrow compensating plate with a width of 10 mm, reduced the stress under tension by 1.2 times for an artificial cutout of a rectangular cross-section, by 1.5 times for an artificial cutout of a triangular cross-section; under torsion, by 3.9 times for a rectangular cross-section of the cutout, 3.5 times for the triangular section of the artificial cutout.

Table 7

Comparison of maximum and critical stresses in bone with different cutout shapes and fixation methods

| Type of cutout | $\sigma_{max}$ when stretched, MPa | | $\tau_{max}$ in torsion, MPa | | Critical stress of the 1st form of lost stability $\sigma_{кр\ 1}$, MPa | |
|---|---|---|---|---|---|---|
| | flat plate | semi-tubular plate | flat plate | semi-tubular plate | no plate and cutout | semi-tubular plate |
| Rectangular cutout | 36.47 | 30.59 | 5.914 | 1.505 | 39.96 | 58.08 |
| Triangular cutout | 47.03 | 30.53 | 5.51 | 1.55 | 46.99 | 61.55 |

Under tension, stress values corresponded to those of intact bone, amounting to 31.59 MPa, while under torsion, values were similar, amounting to 60–70 % of the work of intact bone, equal to 0.757 MPa. A 1.3–1.5-fold increase in critical stress was noted when using a semitubular plate compared to a bone model without curvature or notch. The proposed plate's stability criterion showed higher values than those for intact bone, equal to 54.18 MPa. The semitubular plate could offer better load capacity, both in torsion and tension, than a 10 mm wide flat plate. Load capacity increased with increasing plate thickness. In stretching, specimens with 4 mm of screw penetration performed best; in torsion, specimens with 4 mm and 13 mm of screw penetration performed nearly identically. The specimen with a through-thickness screw penetration resulted in increased stress in the bone at the screw insertion site.

Stress and strain of the *screw-bone* pair model was analyzed to identify mechanisms of screw instability leading to the development of osteosynthesis complications. A study of the stress fields during screw-bone interaction under tangential and axial loading showed that the highest stress concentration in the screw occurred near the head with the shear force from the plate applied (Fig. 6). In bone, the highest stress concentration occurred in the region of maximum stress in the screw, namely, at the screw's entry into the bone.

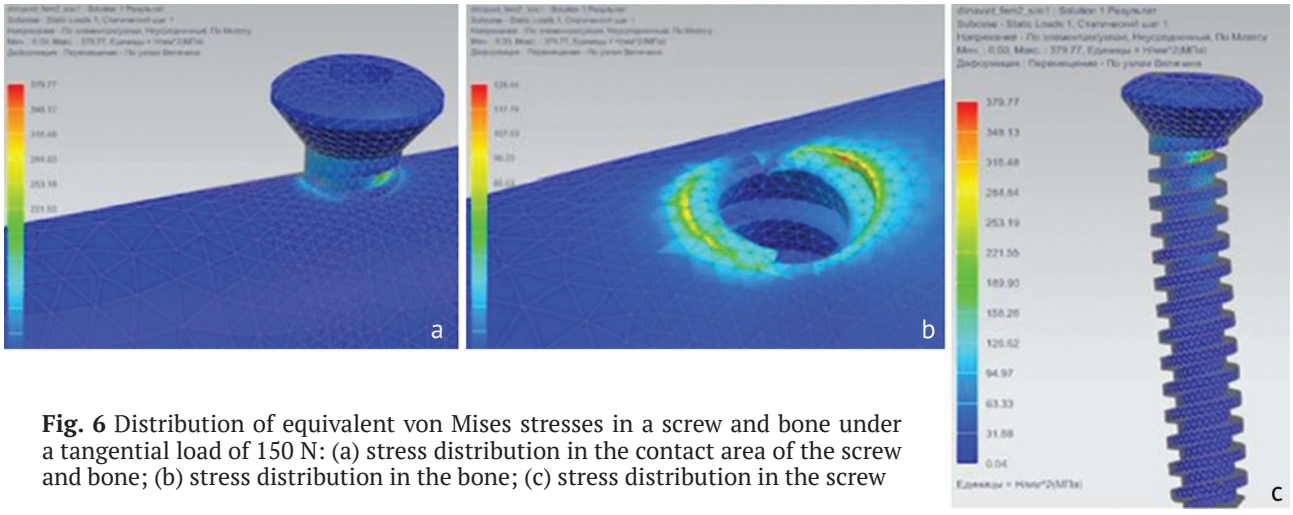


**Fig. 6** Distribution of equivalent von Mises stresses in a screw and bone under a tangential load of 150 N: (a) stress distribution in the contact area of the screw and bone; (b) stress distribution in the bone; (c) stress distribution in the screw

The quantitative parameters of mechanical stresses under shear loads on the screw are presented in Tables 8, 9, and 10. The presented results showed the linear stress dependence on the applied load (Table 8). As the bone layer thickness decreases, the stresses increase. At a thickness of 2.8 mm and a load of 150 N, the bone stress exceeded even the tensile strength of 130 MPa.

A screw was considered short if it passed through one cortex, and long if it passed through both cortices. As the screw length increased, the bone stress increased, and at a load of 150 N, it exceeded the bone's tensile strength (Table 9). The thickness of the cortical bone was taken to be 3.14 mm.

Table 8

Values of equivalent stresses in bone and screw depending on the thickness of the cortical bone under tangential loads

| Load F, H | Stress in the bone σ, MPa | | Stress in the screw σ, MPa | |
|---|---|---|---|---|
| | t = 3,14 mm | t = 2,8 mm | t = 3,14 mm | t = 2,8 mm |
| 50 | 31.13 | 46.52 | 52.41 | 109.92 |
| 100 | 72.26 | 93.04 | 104.82 | 219.84 |
| 150 | 108.39 | 139.1 | 157.23 | 330.49 |

*Note*: t, cortical thickness.

Table 9

Values of equivalent stresses in the bone and screw depending on the screw length under tangential loads

| Load F, H | Stress in the bone σ, MPa | | Stress in the screw σ, MPa | |
|---|---|---|---|---|
| | Short screw | Long screw | Short screw | Long screw |
| 50 | 31.13 | 42.81 | 52.41 | 126.59 |
| 100 | 72.26 | 85.63 | 104.82 | 253.18 |
| 150 | 108.39 | 128.44 | 157.23 | 379.77 |

Table 10

Values of equivalent stresses in the bone and screw depending on the screw diameter under tangential loads

| Load F, H | Stress in the bone σ, MPa | | Stress in the screw σ, MPa | |
|---|---|---|---|---|
| | D = 3.5 mm | D = 4.5 mm | D = 3.5 mm | D = 4.5 mm |
| 50 | 31.13 | 20.51 | 52.41 | 24.27 |
| 100 | 72.26 | 41.02 | 104.82 | 48.54 |
| 150 | 108.39 | 61.53 | 157.23 | 72.81 |

Measurements suggested linear relationship between stress and load applied for screws of different diameters. As the screw diameter increased, the stress in the bone decreased, but even with smaller screw diameters, the stress did not exceed the bone's tensile strength (Table 10). However, a shear load on a screw of 50 N, for most screw parameters and cortical thicknesses, led to increased shear stresses in the bone, exceeding the permissible values, with the exception of a 4.5 mm diameter screw. At higher loads, the permissible values were exceeded in all cases.

There was a linear stress dependence on the shear load applied for various screw parameters (diameter and length) and bone thickness (thickness) facilitating stress prediction under such a load. The stress distribution pattern was the same for all load values. The stress distribution pattern was the same for all load values. The stresses that generated in the bone did not exceed or reach the tensile strength for various screw parameters (length and diameter), but exceeded the tensile strength with a decrease in the thickness of the cortical bone and an increase in the length of the screw under a load of 150 N. The shear stresses increased in the screw and the bone with an increase in the length of the screw.

Under axial loading, the highest stress concentration in the screw was observed at the site of the first three threads, and in the bone, at the entry site of the screw. The maximum stress in the bone depended linearly on the applied axial load on the screw during its tightening. Under a load of 150 N, the maximum equivalent stress in the bone was 88.4 MPa, which exceeded the permissible stress values in the bone leading to a risk of bone destruction and resorption at the contacting plate-bone site with the connection elements and unstable osteosynthesis (Fig. 7). The graph showed that an axial load on the screw exceeding 100 N caused maximum normal stresses in the bone that exceeded their permissible values.

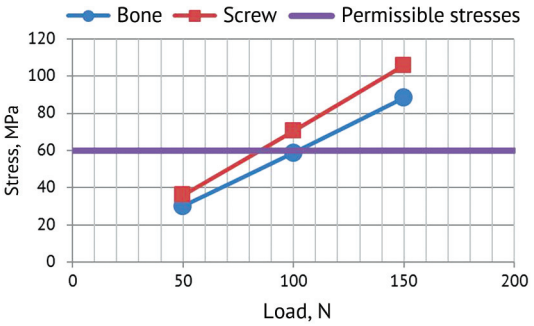


**Fig. 7** Graph of the dependence of the equivalent stress in the bone and screw on the axial load applied

Maximum stresses in the bone depended linearly on the load applied. This allows the obtained results to be extended to other applied loads and predict the stress level under a known load in order to avoid unwanted destruction (local microdestruction) of the cortical bone around the holes and thread stripping due to excessive tightening of the screw. Therefore, the stress and strain of a bone model with a cutout depends on many factors including the type of the loads, methods of defect repair, which should be taken into account in clinical practice for the development of measures to increase the residual strength of the donor radius.

## DISCUSSION

Practical questions reported in the study included how the formation of a notch and the presence of bone curvature in two planes affect the stress and strain of a bone model, what approaches and methods can ensure an increase in the residual strength of the bone and the permissible level of stress in it.

In recent years, the global literature has seen an increase in publications devoted to the application of the finite element method in traumatology and orthopedics, including simulated radial fractures. The method has proven to be very informative in exploring bone strength [16, 17, 25] and it can be used to predict the occurrence and prevention of fractures of the intact radius [16, 17]. It has been established that skeletal models constructed using finite elements provide a non-invasive assessment of the strength and stability of the implant [20]. The authors used computed tomography data from experimental animal bones and artificial bones to construct the FE model. A high degree of correlation between the parameters of the FE model and cadaveric bone was noted [16, 17, 19], which is confirmed by our studies conducted on human anatomical specimens and models based on them. Studies have been published on FE modeling of bone with a marginal defect with the integrity of one of the cortical bones preserved [22]. There are no studies on FE modeling of the radius with a similar defect and compensating elements based on anatomical preparations of human bone using the theory of beam and cross-section bending.

A notch formed in the radial diaphysis model caused a significant increase in the maximum normal stress values compared to the intact bone, which could be explained by a decreased cross-sectional area and the geometric moment of inertia at the notch site. Increased stress indicated a decrease in strength and a greater risk of fracture under real conditions.

Surgeons' opinions regarding the influence of the notch shape on residual bone strength remain controversial. Some authors suggest that a navicular (radial, scaphoid) or keeled (triangular) notch created during graft formation and harvesting can prevent radial fractures, without the use of prophylactic osteosynthesis [26]. Another group of specialists does not see this as necessary, suggesting that it only helps prevent the depth of the incision from being exceeded and improves access and visibility in the surgical area [8, 27, 28].

The extent of the increase in stress depending on the beveling of the osteotomy plane and the increase in the depth of the notch has not been sufficiently explored, and the data are contradictory [28, 29, 30]. The formation of such a notch can be accompanied by a minimal effect and lead to an increase in bone torsional strength of 5 % only [28, 29], while others report a significant positive effect of the osteotomy shape on bending and torsional strength [30]. Our data are consistent with the results of the TEM of other authors, with the peak stress values in four-point bending and torsion being 24–30 % higher with a rectangular osteotomy than with a beveled one [30]. This result can be explained by the fact that a rectangular cutout has two stress concentrators at the corners of the defect, while a triangular cutout has one, with a lower stress concentration coefficient. Theoretically, a radius (boat-shaped, shuttle-shaped) cutout would have an even lower stress concentration by rounding (smoothly changing the shape) the notch in the narrowest part of the remaining bone. However, the normal stress in the bone was still higher in the case than the permissible values, and therefore the formation of a triangular or radial notch must be combined with other strengthening methods [28]. Increased depth of the notch led to a disproportionate increase in stress in the bone, especially during torsion, regardless of the shape of the notch [30]. The role of bone bending in the genesis of the stress and strain has not been explored. Our findings showed that the presence of bone curvature led to an increase in normal tensile stresses by almost three times compared to a bone model without

curvature. The increase in tensile-compressive stress in the presence of bone curvature can be explained by the occurrence of a longitudinal bending moment due to the occurrence of eccentric forces with the severity being dependent on the magnitude of the bending, which was proven by the method of mathematical modeling [31]. The presence of a notch combined with a bone curvature weakens the bone significantly according to the principle of superposition of forces,with normal tensile stresses and bending stresses caused bythe presence of a bend and a bone defect being summed up. This is confirmed by distribution of voltage fields.

The longitudinal stability of the notched bone remains unexplored. In real-world conditions, this type of impact can occur under axial loading (compression) on the forearm during a fall or impact. We believe that the loss of longitudinal stability of the notched bone occurs due to the reduction of the geometric moment of inertia of the section and the presence of the initial curvature of the bone, which leads to the eccentricity of the compressive and tensile forces, that is, to eccentric tension and compression. The presence of the notch can lead to eccentricity of the force and the occurrence of a bending moment. The greater margin of safety of a bone with a triangular notch in terms of longitudinal stability compared to a rectangular notch is explained by the weakening of its cross-section over a greater length with the moment of inertia of the section of the bone is less at the rectangular cut.

There are reports on the increased strength of the radius with a marginal defect fixed with a bone bridge plate under bending and torsion conditions [6, 18, 21, 28]. The influence of flat straight and T-shaped plates on the stress and strain of a finite element model of a bone with a marginal notch was explored [22]. However, the mechanisms by which maximum bone stress changes when using other types of plates, including semitubular ones, have not been studied. At the current stage of reconstructive surgery, the size, placement of the plate, the number and size of fixation screws, and the method of their placement have also not been definitively determined. There is no data on the comparative analysis of the effectiveness of options for prophylactic osteosynthesis of bone with a marginal defect using FEM under different types of loading [8, 21]. Quantitative analysis of the stress fields of the model with a plate showed that fixation with a 2 mm thick plate on four screws (two on each side of the defect) with a diameter of 2.0 mm, inserted bicortically, is sufficient to reduce the stress in the bone, since they do not exceed the permissible values in this case, although they are close to them. There is a slight decrease in the stress in the bone with a thicker plate and more screws. Increased number of screws and, consequently, the plate length in clinical settings leads to increased duration, increased invasiveness, and the risk of impaired bone circulation. The results can be explained by the fact that the cross-sectional area is the measure of plate stiffness under simple tension and compression. Increasing the plate thickness from 1 mm to 2 mm doubles the cross-sectional area, and the stiffness, while increasing it from 2 mm to 3 mm increases it by a third. For this reason, a 2 mm thick plate can be used, as the stress in the bone decreases only slightly compared to a 3 mm thick plate. The excess of permissible bone stress in the model with a 1 mm thick plate can be explained by insufficient rigidity of the plate and the high stress within it with resultant greater stress in the bone.

The number of fixing screws required can also be justified through a qualitative analysis of the model's stress fields. A study of the influence of the number of fixing screws, their location, and plate thickness on the nature of stress distribution in various elements of the model showed that the primary load during prophylactic bone strengthening with a plate is borne by the fixation plate and the remaining cortical layer of the radius in the notch area. These areas of bone have reduced load-bearing capacity, and the load from them is transferred to the reinforcing plate via screws outside the notch increasing the strength of the defect. With the screws adequately placed, the tensile-compressive load between them depends on their number: the more screws, the less stress being applied to the screws and bone material. If the screws are arranged in a longitudinal row and there is little friction between the plate and the bone material, the load on each screw will depend on the distance between the screws and their distance from the defect.

The presence of friction between the plate and bone will theoretically reduce the load on the screws, as some of it will be absorbed by the friction surfaces. However, with a smooth contact surface of the supporting plate, this reduction may be insignificant. The areas of the reinforcing plate

in the cutout area and the screws closest to the defect were the most heavily loaded due to their location near the weakened portion of the bone. This can be explained by their location in a zone of high stress due to their location near the bone with a reduced cross-section and, consequently, lower rigidity, experiencing the greatest deformations (longitudinal and angular displacements) and stresses together with the plate in the cutout area compared to intact areas. The stresses will be lower in the pair of screws next to the defect and in the presence of a third pair of screws, even lower, which is consistent with the results of other studies conducted using FEM [22]. With three or more screws, the primary load is supported by the first two screws, while subsequent screws bear significantly lighter loads and are therefore ineffective. The greatest stress relaxation occurred in the area of the two end screws. This stress distribution in the screws during tension-compression in the calculation model can be explained not only by the presence of a weakened bone area, as well as misalignment of the bone and supporting plate axes and the occurrence of eccentric forces leading to bone bending and rotation. The findings are consistent with the results of other studies conducted with FEM to analyze the stress distribution between screws on a model of a diaphyseal fracture fixed with a dynamic compression plate (DCP) and a fixation compression plate with angular stability (LCP) as well as when exploring long-term results of extracorporeal osteosynthesis of long tubular bones with radiographs [18, 22].

Under torsional loads, the stress in the bone is lower than the permissible value, even for a 1 mm thick plate. This is because the plate significantly reduces the torsional angle due to its rigidity, so the number of screws and the plate thickness have little effect on the stress magnitude. However, in the case of using flat plates when fastened with one screw on each side, a single screw does not prevent rotation and possible shifting of the plate under loading, which is excluded when fixing with two screws on each side of the defect or using a semi-tubular plate.

The maximum shear stress occurring in the plate can be observed in the screws closest to the defect. With greater number of screws, the torsion angle decreases due to the increased stiffness of the connection. As the plate thickness increases, the stress within it decreases and is little affected by the number of screws, which can be explained by the increased cross-sectional area of the model and the strength (rigidity due to the high modulus of elasticity of the metal) of the connection. Fastening with fewer screws (one on each side) is ineffective for torsional load, even when installing such plates. When the bone is twisted, the load distribution between the screws is different, and it can be assumed that when fastening with two pairs of screws, the torsional rigidity of the resulting section can be sufficient, since the twisting angles are small and an increase in the number of screws has little effect on these parameters. Taking these facts into account, it can be assumed that fixation with a narrow plate 2 mm thick on four screws 4 mm in diameter provides sufficient strength even under tangential loads on the calculation model.

An analysis of the stress distribution in various elements of our *bone–screw–plate* model showed that the greatest stresses were obtained in the plate, and the least in the screws during tension–compression and torsion of the bone. This result can be explained by the fact that screws are subject to predominantly shear stresses, which are typically lower than normal stresses. The screw-contact zone in the plate is subject to predominantly normal bearing stresses, while normal and shear stresses are present in the bone. As plate thickness increases, stresses in the structural elements decrease linearly. Increasing plate thickness would lead to increased fixation rigidity in clinical settings causing a "stress-shielding" effect, weakening of the bone [6, 32, 33] and plate protrusion above soft tissue or prolapse [33]. This can be accompanied by greater trauma of the intervention, the risk of damage to muscles, nerves, blood vessels, impaired bone circulation and the development of infectious complications [34].

The plate's lower profile would occupy minimal tissue volume in real-world conditions, facilitating suturing of the tissues above the plate without tensioning the wound edges. The plates may offer a potential advantage over 3.5 mm thick plates in accelerating fracture healing due to reduced stress shielding, allowing forces to be distributed evenly along the length. Experimental studies on a composite anatomical model of the forearm bone demonstrated plastic deformation of the low-profile plate without fracture, thanks to its flexibility despite excessive loads which potentially prevents re-fracture observed with the use of thicker plates [33].

The advantages we have identified with a semi-tubular plate over a flat narrow plate can be explained by the fact that a bone model with a plate shaped to envelop the cylindrical surface of the bone bears a greater load due to the increased rigidity of the connection in two directions due to the shape of the metal construct. Increasing the plate thickness leads to a reduced stress in all elements of the *bone-screw-plate* system, since the area and moment of inertia of the cross-section of the joint increase. This plate, compared to a narrow straight plate, reduces the level of stress in the bone to a greater extent during tension and torsion (the main mechanism contributing to the fracture, in which the load on the radius cannot be absorbed by the ulna). According to the longitudinal stability criterion, the triangular-notched bone reinforced with the plate exhibits higher critical stress values than the intact bone. The triangular-notched bone model reinforced with the plate exhibits higher critical stress values than the rectangular-notched model and a similar plate in longitudinal bending and torsion suggesting the practical use of a triangular cutout in combination with prophylactic fixation with a bone plate. It can be assumed that similar patterns can occur with other types of loads. This is consistent with the surgeons' opinion on the need to bevel the corners of the cut and shape it triangular or scaphoid in combination with prophylactic bone plating [8, 22]. With the residual strength of the radius increased with plate fixation a larger cross-section of bone can be harvested allowing reconstruction of a larger defect without the risk of the radius fracture. A graft thickness not exceeding 1/2 the diameter or the bone circumference can be harvested without prophylactic bone fixation [6, 21].

There are isolated reports of successful fracture prevention by replacing the defect with an autogenous bone insert fixed with screws. According to our data, replacing a rectangular defect with a compensating insert without prophylactic plating does not provide adequate stress reduction in the bone, and high stress concentration values remain in the corners of the cutout for the period of insert consolidation.

The strength of the screw-bone connection is crucial for ensuring the stability of bone plating. The problem of screw instability during metal osteosynthesis remains a pressing issue. Screw loosening is the most common complication of plating. Screw loosening leads to serious complications, failed plating and bone fractures. are poorly understood. Microcracks, bone fractures at the screw site, bone resorption caused by excessive stress in the perifocal bone surrounding the screw are most common mechanisms underlying this phenomenon. This raises the question of the parameters and placement of plate-fixing screws to ensure the necessary bone strength. Some authors report the advantages of bicortical fixation [6, 8], while others report the advantages of monocortical screw placement [24, 35]. We analyzed the stresses and deformations of the bone and screw at the connection site depending on the diameter, length of the screw, and the thickness of the cortical layer. Mechanisms of screw instability, the strength of screw pull-out or screw-in under axial load was explored on experimental models made from different artificial (synthetic) materials, including bone plating [36, 37, 38, 39, 40] and using the FE method [41, 42, 43].

Our findings showed that pure tension-compression and torsion caused the main load on the screws fixing the plate as the shear load from the plate, causing shear stresses. The bone also experienced bending from the longitudinal load due to the existing curvature, so the normal load transmitted from the reinforcing rigid plate to the screw is added to the shear, tending to tear the screws out of the bone when there was a significant difference in the bending rigidity of the bone (especially the damaged area) and the plate. When the plate was placed on the convex side of a curved bone, such a pull-out load occurred under compression and under tension on a concave side. The load was greater with the screw being closer to the apex of the bone's curve. For this reason, the tangential loads on the screw and the axial loads in the screw-bone contact pair at the bone-screw interface were explored. We found that the tangential stresses, and consequently the bone deformation, increased with increasing screw length, decreasing screw diameter and decreasing cortical bone thickness. The findings can be interpreted as follows. Increasing the contact area of the screw-bone pair leads to a decrease in stress in all elements of the screw-bone-plate system. The lowest stress in the bone was observed in the model with monocortical insertion of a short screw (3.5–4.0 mm). The lower level of shear stresses with short screws fastened through one cortex may be due to the shorter length, due to which the screw practically does not bend and a lower bending moment is generated under tangential loading. The screw penetrated by 3.5–4.0 mm provides less secure plate attachment due a greater risk

of screw to be torn out of the bone under tension, especially if the bone is curved. A larger contact screw and the bone area would provide greater strength and rigidity either by increased thickness of the cortical layer, the diameter of the screws, or by increasing their number, length and placing the screws through both cortices. The stresses in the screw during this procedure may be somewhat higher due to the increased arm of the tangential force applied from the plate, despite the increased area of the screw contraction with the bone. A long screw traverses two cortices and can bend under shear load on the head, increasing the stress due to the bending moment. In practice, this necessitates a tradeoff between the greater invasiveness of the surgery and the reduced risk of plate detachment due to screw pullout. An increased thickness of the cortex can lead to decreased stress in all elements of the screw-bone system with the contact area of the screw-bone pair increased.

With a thinner cortex, the contact area with the screw decreases leading to increased stress, which is more significant than with changes in screw parameters. Based on the facts, it can be concluded that a decreased thickness of the cortex, which is more common in osteoporosis in women is associated with increased number, diameter, length of screws and thickness of the plate increasing the screw-bone contact area, and ultimately, the strength and rigidity of fixation. Due to the fact that a normal axial load is transferred from the plate to the screw during stretching and compression of the bone, which tends to pull out the screw, its bicortical placement is practical especially in cases of large curvature of the bone and the close location of the screw or defect to the apex of the curvature. Tangential and normal stresses acting on a screw are essential for identifying instability mechanisms [44, 45]. Our results are consistent with the literature data, suggesting radial and axial stresses acting on the screw fixing the plate [18, 44, 45]. In this case, shear stresses play a leading role in screw loosening, since the volume of bone resorption in the perifocal area appear to be greater under radial loading than axial loading for all types of loading [18]. For this reason, the primary indicator of screw loosening risk may be its shear resistance rather than axial pullout strength. According to the researchers, radial screw resistance is more associated with physiological craniocaudal loads,and the strength of the screw under axial load mainly determines the ability of the bone to resist torsion [18, 44]. Higher values of tangential and normal stresses for the perifocal bone at the site of insertion of the central screws indicate the potential for primary resorption, bone damage and, ultimately, loosening or fracture of the screws. According to available literature, bone resorption is caused by mechanical stress exceeding the bone's tensile strength. According to other authors, the critical threshold for bone resorption is approximately 50 MPa, which is lower than the ultimate strength of the cortical layer of the normal radius bone under torsion [18]. The data were obtained using a FE model of the tibial diaphysis fixed with a plate and by analyzing radiographs of long bones after plating [18]. According to our data, placement of screws into the bone is associated with resorption or destruction of bone tissue in the perifocal area in case of exceeded longitudinal (axial) load, equal to 100 N with the permissible stress (60 MPa) almost reached and a decreased thickness of the cortical layer. Stable fixation of the two central screws experiencing the greatest shear stresses can be provided by increasing the diameter and length for bicortical placement, especially with large bone curvature and decreased thickness of the cortical layer. In practice, maximum caution is needed for screw placement without exceeding the permissible axial load, avoiding unwanted damage to the cortex.

Therefore, the SS model of the radial diaphysis allowed us to understand mechanisms of strength reduction, obtain an idea of the residual strength of the bone after the formation of rectangular and triangular marginal notches, and the use of various methods for compensating for the defect and preventing pathological fracture. The findings can be extrapolated to the clinic, with a certain degree of conventionality, for the development of methods for the prevention and treatment of patients with fractures of the osteotomized radius, since they provide an idea of the strength properties of the bone and the mechanisms for achieving screw stability when fixing it with a plate. We believe that internal fixation of the radius with a plate and screws can prevent fractures, resulting in reduced morbidity to acceptable levels, which will expand the indications for the use of RFFF in many areas of surgery.

## CONCLUSION

The presence of a notch and bone curvature in two planes significantly increased the level of normal mechanical stress in the bone model. The bone model with a triangular notch exhibited lower stress levels than the model with a rectangular notch. The findings substantiated the need to strengthen the radius shaft with a marginal notch using a bone plate, regardless of a shape, which will reduce the mechanical stress on the bone below the permissible level. Bone models with a semitubular plate demonstrated an advantage over models with a flat narrow plate providing a greater reduction in stress levels. Bone stress decreased with increasing cortical and plate thickness, and with the number and diameter of screws.

***Conflict of interest*** *None of the authors has any potential conflict of interest.*

***Funding*** *The authors received no specific funding for this work.*

## REFERENCES

1. Silverman DA, Przylecki WH, Shnayder Y, et al. Expanding the Utilization of the Osteocutaneous Radial Forearm Free Flap beyond Mandibular Reconstruction. *J Reconstr Microsurg*. 2016;32(5):361-365. doi: 10.1055/s-0035-1571251.
2. Chappell AG, Ramsey MD, Dabestani PJ, Ko JH. Vascularized Bone Graft Reconstruction for Upper Extremity Defects: A Review. *Arch Plast Surg*. 2023;50(1):82-95. doi: 10.1055/s-0042-1758639.
3. Kearns M, Ermogenous P, Myers S, Ghanem AM. Osteocutaneous flaps for head and neck reconstruction: A focused evaluation of donor site morbidity and patient reported outcome measures in different reconstruction options. *Arch Plast Surg*. 2018;45(6):495-503. doi: 10.5999/aps.2017.01592.
4. Archibald H, Stanek J, Hamlar D. Free Flap Donor-Site Complications and Management. *Semin Plast Surg*. 2022;37(1):26-30. doi: 10.1055/s-0042-1759795.
5. Clark S, Greenwood M, Banks RJ, Parker R. Fracture of the radial donor site after composite free flap harvest: a ten-year review. *Surgeon*. 2004;2(5):281-286. doi: 10.1016/s1479-666x(04)80098-2.
6. Avery CM, Parmar S, Martin T. The use of a T-shaped contoured unilocking titanium radial plate for prophylactic internal fixation of the radial osteocutaneous donor site. *Br J Oral Maxillofac Surg*. 2010;48(8):648-650. doi: 10.1016/j.bjoms.2010.01.013.
7. Werle AH, Tsue TT, Toby EB, Girod DA. Osteocutaneous radial forearm free flap: its use without significant donor site morbidity. *Otolaryngol Head Neck Surg*. 2000;123(6):711-717. doi: 10.1067/mhn.2000.110865.
8. Shnayder Y, Tsue TT, Toby EB, et al. Safe osteocutaneous radial forearm flap harvest with prophylactic internal fixation. *Craniomaxillofac Trauma Reconstr*. 2011;4(3):129-136. doi: 10.1055/s-0031-1279675.
9. Tankersley A, Velasco Martinez I, Medina A. Use of cervicothoracic rotation flap and osteocutaneous radial forearm free flap for a complex multilayered cheek defect reconstruction. *Case Reports Plast Surg Hand Surg*. 2020;7(1):98-104. doi: 10.1080/23320885.2020.1806070.
10. Loeffelbein DJ, Al-Benna S, Steinsträßer L, et al. Reduction of donor site morbidity of free radial forearm flaps: what level of evidence is available? *Eplasty*. 2012;12:e9.
11. Waits CA, Toby EB, Girod DA, Tsue TT. Osteocutaneous radial forearm free flap: long-term radiographic evaluation of donor site morbidity after prophylactic plating of radius. *J Reconstr Microsurg*. 2007;23(7):367-372. doi: 10.1055/s-2007-992342.
12. Silverman DA, Przylecki WH, Arganbright JM, et al. Evaluation of bone length and number of osteotomies utilizing the osteocutaneous radial forearm free flap for mandible reconstruction: An 8-year review of complications and flap survival. *Head Neck*. 2016;38(3):434-438. doi: 10.1002/hed.23919.
13. Pimenov SA. Application of NX nastran for reliability assessment of metal structures. *J Sc Intensive Technol*. 2012;(5):70-76. (In Russ.)
14. Omarov MD, Muslimova FN. Analytical review of the methodology of computer modeling. *Int J Applied Fundamental Research*. 2015;(3-1):11-14. (In Russ.) URL: https://applied-research.ru/ru/article/view?id=6466.
15. Edwards WB, Troy KL. Finite element prediction of surface strain and fracture strength at the distal radius. *Med Eng Phys*. 2012;34(3):290-298. doi: 10.1016/j.medengphy.2011.07.016.
16. Matsuura Y, Kuniyoshi K, Suzuki T, et al, Takahashi K. Accuracy of specimen-specific nonlinear finite element analysis for evaluation of distal radius strength in cadaver material. *J Orthop Sci*. 2014;19(6):1012-1018. doi: 10.1007/s00776-014-0616-1.
17. Jiang H, Robinson DL, McDonald M, et al. Predicting experimentally-derived failure load at the distal radius using finite element modelling based on peripheral quantitative computed tomography cross-sections (pQCT-FE): A validation study. *Bone*. 2019;129:115051. doi: 10.1016/j.bone.2019.115051.
18. Feng X, Lin G, Fang CX, et al. Bone resorption triggered by high radial stress: The mechanism of screw loosening in plate fixation of long bone fractures. *J Orthop Res*. 2019;37(7):1498-1507. doi: 10.1002/jor.24286.
19. Liu J, Mustafa AK, Lees VC, et al. Analysis and validation of a 3D finite element model for human forearm fracture. *Int J Numer Method Biomed Eng*. 2022;38(9):e3617. doi: 10.1002/cnm.3617.
20. Campbell GM, Glüer CC. Skeletal assessment with finite element analysis: relevance, pitfalls and interpretation. *Curr Opin Rheumatol*. 2017;29(4):402-409. doi: 10.1097/BOR.0000000000000405.
21. Bowers KW, Edmonds JL, Girod DA, et al. Osteocutaneous radial forearm free flaps. The necessity of internal fixation of the donor-site defect to prevent pathological fracture. *J Bone Joint Surg Am*. 2000;82(5):694-704.
22. Avery CM, Bujtár P, Simonovics J, et al. A finite element analysis of bone plates available for prophylactic internal fixation of the radial osteocutaneous donor site using the sheep tibia model. *Med Eng Phys*. 2013;35(10):1421-1430. doi: 10.1016/j.medengphy.2013.03.014.

23. Roberts JW, Grindel SI, Rebholz B, Wang M. Biomechanical evaluation of locking plate radial shaft fixation: unicortical locking fixation versus mixed bicortical and unicortical fixation in a sawbone model. *J Hand Surg Am*. 2007;32(7):971-975. doi: 10.1016/j.jhsa.2007.05.019.
24. Overturf SJ, Morris RP, Gugala Z, Lindsey RW. Biomechanical comparison of bicortical locking versus unicortical far-cortex-abutting locking screw-plate fixation for comminuted radial shaft fractures. *J Hand Surg Am*. 2014;39(10):1907-1913. doi: 10.1016/j.jhsa.2014.06.141.
25. Hosseini HS, Dünki A, Fabech J, et al. Fast estimation of Colles' fracture load of the distal section of the radius by homogenized finite element analysis based on HR-pQCT. *Bone*. 2017;97:65-75. doi: 10.1016/j.bone.2017.01.003.
26. Thoma A, Khadaroo R, Grigenas O, et al. Oromandibular reconstruction with the radial-forearm osteocutaneous flap: experience with 60 consecutive cases. *Plast Reconstr Surg*. 1999;104(2):368-378; discussion 379-80. doi: 10.1097/00006534-199908000-00007.
27. Swanson E, Boyd JB, Mulholland RS. The radial forearm flap: a biomechanical study of the osteotomized radius. *Plast Reconstr Surg*. 1990;85(2):267-272.
28. Avery CM, Best A, Patterson P, et al. Biomechanical study of prophylactic internal fixation of the radial osteocutaneous donor site using the sheep tibia model. *Br J Oral Maxillofac Surg*. 2007;45(6):441-446. doi: 10.1016/j.bjoms.2006.10.010.
29. Meland NB, Maki S, Chao EY, Rademaker B. The radial forearm flap: a biomechanical study of donor-site morbidity utilizing sheep tibia. *Plast Reconstr Surg*. 1992;90(5):763-773.
30. Bujtar P, Simonovics J, Váradi K, et al. Refinements in osteotomy design to improve structural integrity: a finite element analysis study. *Br J Oral Maxillofac Surg*. 2013;51(6):479-485. doi: 10.1016/j.bjoms.2012.09.015.
31. Aleksandrov NM, Veshutkin VD, Zhukov AE, et al. The application of mathematical simulation for studying the strength properties of a donor radius. *Russian Journal of Biomechanics*. 2017;21(2):147-165. (In Russ.) doi: 10.15593/RZhBiomeh/2017.2.03.
32. Hirashima T, Matsuura Y, Suzuki T, et al. Long-term Evaluation Using Finite Element Analysis of Bone Atrophy Changes after Locking Plate Fixation of Forearm Diaphyseal Fracture. *J Hand Surg Glob Online*. 2021;3(5):240-244. doi: 10.1016/j.jhsg.2021.05.013.
33. Wahbeh JM, Kelley BV, Shokoohi C, et al. Comparison of a 2.7-mm and 3.5-mm locking compression plate for ulnar fractures: a biomechanical evaluation. *OTA Int*. 2023;6(3):e278. doi: 10.1097/OI9.0000000000000278.
34. Zhao X, Jing W, Yun Z, et al. An experimental study on stress-shielding effects of locked compression plates in fixing intact dog femur. *J Orthop Surg Res*. 2021;16(1):97. doi: 10.1186/s13018-021-02238-3.
35. Shanmugam R, Jian CYCCS, Haseeb A, Aik S. Comparing biomechanical strength of unicortical locking plate versus bicortical compression plate for transverse midshaft metacarpal fracture. *J Orthop Surg (Hong Kong)*. 2018;26(3):2309499018802511. doi: 10.1177/2309499018802511.
36. Bronsnick D, Harold RE, Youderian A, et al. Can high-friction intraannular material increase screw pullout strength in osteoporotic bone? *Clin Orthop Relat Res*. 2015;473(3):1150-1154. doi: 10.1007/s11999-014-3975-1.
37. Wang T, Boone C, Behn AW, et al. Cancellous Screws Are Biomechanically Superior to Cortical Screws in Metaphyseal Bone. *Orthopedics*. 2016;39(5):e828-e832. doi: 10.3928/01477447-20160509-01.
38. Jazini E, Petraglia C, Moldavsky M, et al. Finding the right fit: studying the biomechanics of under-tapping with varying thread depths and pitches. *Spine J*. 2017;17(4):574-578. doi: 10.1016/j.spinee.2016.11.019.
39. Varghese V, Saravana Kumar G, Krishnan V. Effect of various factors on pull out strength of pedicle screw in normal and osteoporotic cancellous bone models. *Med Eng Phys*. 2017;40:28-38. doi: 10.1016/j.medengphy.2016.11.012.
40. Wu LC, Hsieh YY, Tsuang FY, et al. Pullout strength of different pedicle screws after primary and revision insertion: an in vitro study on polyurethane foam. *BMC Musculoskelet Disord*. 2023;24(1):863. doi: 10.1186/s12891-023-07015-3.
41. Geng JP, Ma QS, Xu W, et al. Finite element analysis of four thread-form configurations in a stepped screw implant. *J Oral Rehabil*. 2004;31(3):233-239. doi: 10.1046/j.0305-182X.2003.01213.x.
42. Eraslan O, Inan O. The effect of thread design on stress distribution in a solid screw implant: a 3D finite element analysis. *Clin Oral Investig*. 2010;14(4):411-416. doi: 10.1007/s00784-009-0305-1.
43. Oswal MM, Amasi UN, Oswal MS, Bhagat AS. Influence of three different implant thread designs on stress distribution: A three-dimensional finite element analysis. *J Indian Prosthodont Soc*. 2016;16(4):359-365. doi: 10.4103/0972-4052.191283.
44. Feng X, Qi W, Zhang T, et al. Lateral migration resistance of screw is essential in evaluating bone screw stability of plate fixation. *Sci Re*p. 2021;11(1):12510. doi: 10.1038/s41598-021-91952-3.
45. Feng X, Luo Z, Li Y, et al. Fixation stability comparison of bone screws based on thread design: buttress thread, triangle thread, and square thread. *BMC Musculoskelet Disord*. 2022;23(1):820. doi: 10.1186/s12891-022-05751-6.

The article was submitted 04.02.2025; approved after reviewing 21.04.2025; accepted for publication 14.10.2025.

**Information about the authors:**

Nikolay M. Aleksandrov — Doctor of Medical Sciences, Leading Researcher, aleksandrov-chetai@rambler.ru;

Vladimir D. Veshutkin — Candidate of Technical Sciences, Associate Professor of the Department;

Aleksandr E. Zhukov — Candidate of Technical Sciences, Associate Professor of the Department;

Ivan D. Veshaev — Postgraduate Student.